29th International Cosmic Ray Conference Pune (2005) **6**, 89-92

Simulation of the ATIC-2 Silicon Matrix for Protons and Helium GCR Primaries at 0.3, 10, and 25 TeV/nucleon

J. Watts[a], J. H. Adams[a], G. Bashindzhagyan[b], K. E. Batkov[c], J. Chang[d], M. Christl[a], A. R. Fazely[e], O. Ganel[e], R. M. Gunasingha[e], T. G. Guzik[b], J. Isbert[b], K. C. Kim[f], E. Kouznetsov[g], M. Panasyuk[c], A. Panov[c], W. K. H. Schmidt[c], E. S. Seo[f], R. Sina[f], N. V. Sokolskaya[c], J. Z. Wang[f], J. P. Wefel[b], J. Wu[f] and V Zatsepin[c]
(a) XD12 Marshall Space Flight Center, Huntsville, AL 35812, USA
(b) Louisiana State University, Baton Rouge, LA, USA
(c) Skobeltsyn Institute of Nuclear Physics, Moscow State University, Moscow, Russia
(d) Max Plank Institute fur Aeronomie, Lindau, Germany
(e) Southern University, Baton Rouge, LA, USA
(f) University of Maryland, College Park, MD, USA
(g) University of Alabama-Huntsville, Huntsville, AL, USA
Presenter: J. Watts (john.w.watts@nasa.gov), usa-watts-J-abs3-he11-oral

The energy deposition distribution for protons and helium galactic cosmic ray primaries at 0.3, 10, and 25 TeV/nucleon in the ATIC-2 silicon matrix detector are simulated with GEANT4.

1. Introduction

The GEANT3 geometrical model of ATIC developed by the University of Maryland was combined with a GEANT4 application developed for the Deep Space Test Bed (DSTB) detector package. The new code included relatively minor modifications to completely describe the ATIC materials and a more detailed model of the Silicon Matrix detector. For this analysis all particles were started as a unidirectional beam at a single point near the center of the Silicon Matrix front surface. The point was selected such that each primary passed through at least two of the overlapping silicon pixels.

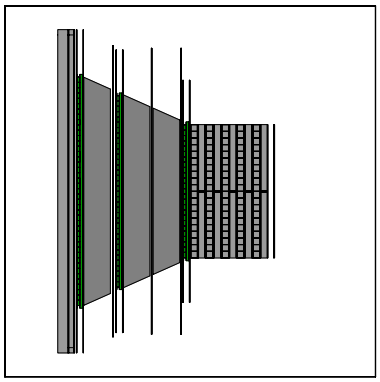

Figure 1. ATIC GEANT4 Geometry model. (The Silicon Matrix is at the left.)

2. Discussion

The starting primaries were mono-energetic with energies 0.3, 10, and 25 TeV/nucleon. 100000 primaries were started for each sample run. Figures 2 through 7 show the distribution of energy deposited in the first

silicon pixel encountered for normal incidence. The key conclusion from these plots is that the GEANT4 simulation shows no significant energy dependence of the energy deposition over the energy range selected. The mean and RMS of the corresponding distributions are same within statistics from 0.3 TeV to 25 TeV/nucleon.

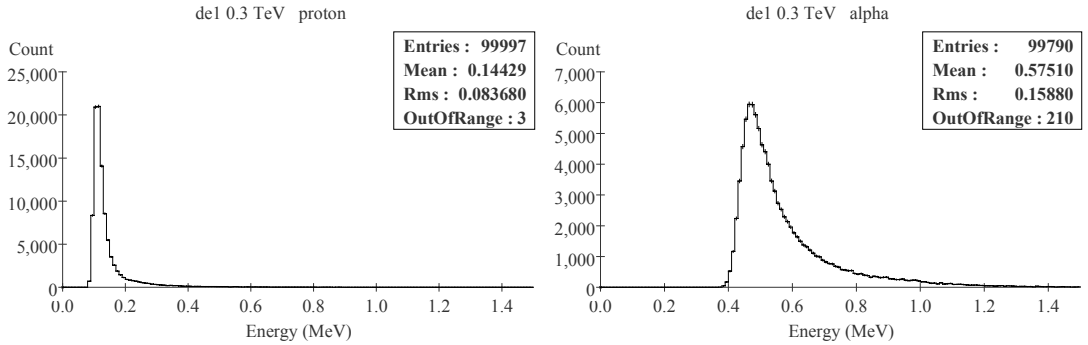

Figure 2. Energy deposition in the first silicon pixel encountered at a primary particle kinetic energy of 0.3 TeV/nucleon. The left graph is for protons, and the right graph is for helium nuclei.

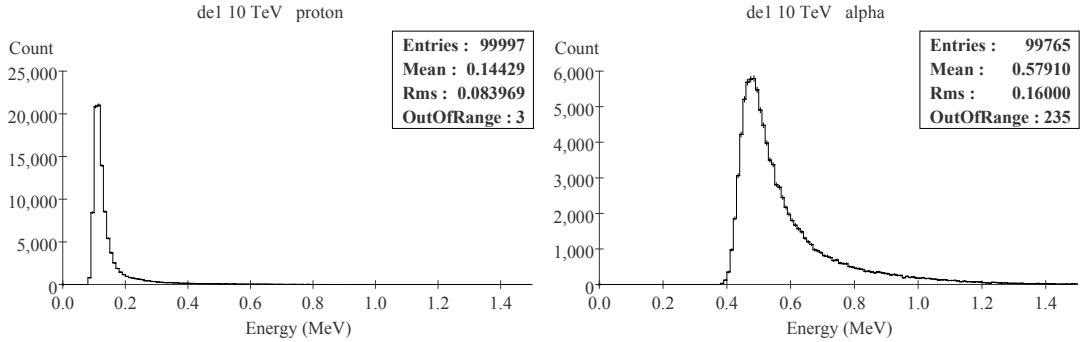

Figure 3. Energy deposition in the first silicon pixel encountered at a primary particle kinetic energy of 10 TeV/nucleon. The left graph is for protons, and the right graph is for helium nuclei.

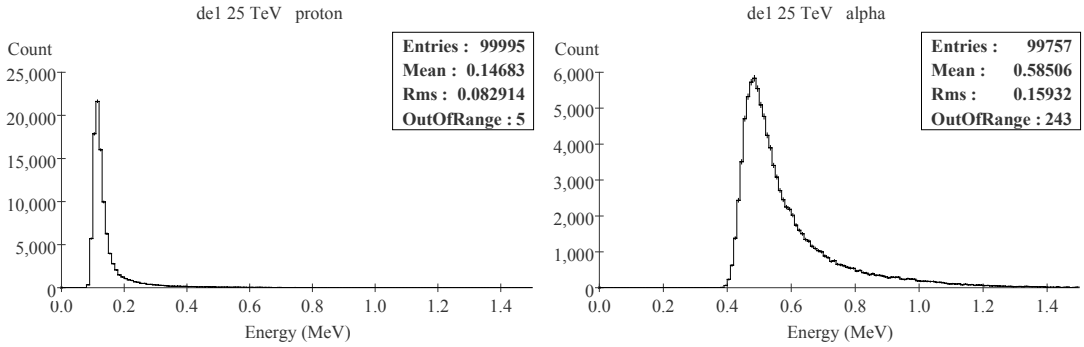

Figure 4. Energy deposition in the first silicon pixel encountered at a primary particle kinetic energy of 25 TeV/nucleon. The left graph is for protons, and the right graph is for helium nuclei.

Flight measurements of the electron noise in the silicon matrix and front-end electronics are well represented by normal distribution with a variance of 0.4MIPS (~58 keV)[1]. Figure 5 shows the distribution of the

energy deposited plus 58 keV of electronic noise in the first pixel at 10 TeV/nucleon. Table 1 show the misidentification fraction as a function of energy deposition.

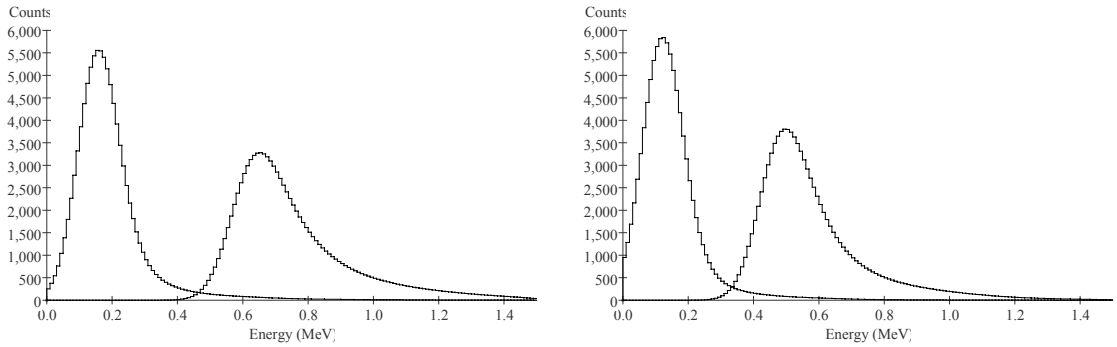

Figure 5. The energy deposition including 58 keV of electronic noise in the first pixel encountered at 10 TeV/nucleon. Distribution for both protons and helium nuclei are shown. (The left plot is for normal incidence and the right plot is for 40° incidence.)

Table 1. Misidentification fraction where protons are required to have the silicon pixel energy depositions above D and Helium nuclei are required to have the silicon pixel energy deposition below D.

	0° incidence		40° incidence	
D (MeV)	Proton	Helium	Proton	Helium
0.2	0.186	0.0	0.351	0.0
0.3	0.053	0.002	0.099	0.0
0.4	0.026	0.063	0.046	0.0
0.5	0.014	0.364	0.027	0.016
0.6	0.008	0.680	0.016	0.172

The ATIC silicon matrix has multiple pixel coverage for about 20% of the front surface. For the sampled runs the starting point and direction were selected so that each primary passes through at least two silicon pixels. With two samples of energy deposition protons can be more easily separated from helium nuclei. Figure 6 shows the distribution of the average of energy deposited in the first and second pixel at 10 TeV/nucleon include 58 keV of electronic noise. Table 2 shows the misidentification fraction as a function of D.

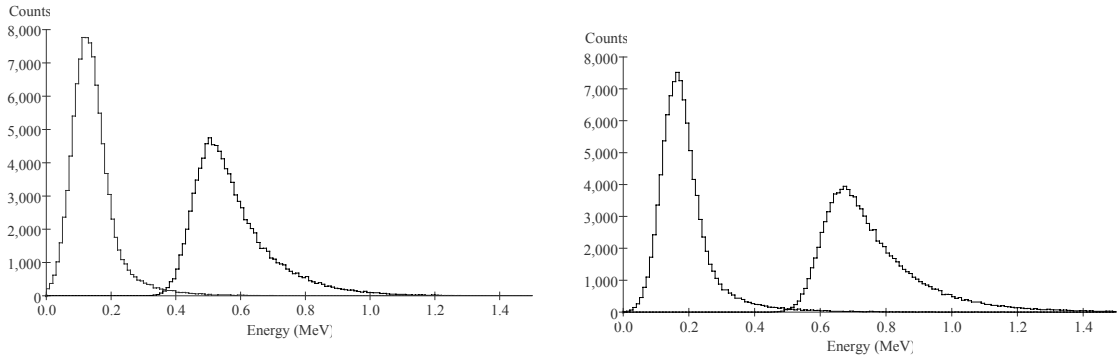

Figure 6. The average of the energy deposition in the first and second pixel encountered at 10 TeV/nucleon including 58 keV of electronic noise. Distribution for both protons and helium nuclei are shown. (The left plot is for normal incidence and the right plot is for 40° incidence.)

Table 2. Misidentification fraction where protons are required to have the average of both silicon pixel energy depositions above D and Helium nuclei are required to have the average of both silicon pixel energy depositions below D.

	0° incidence		40° incidence	
D (MeV)	Proton	Helium	Proton	Helium
0.2	0.145	0.0	0.324	0.0
0.3	0.034	0.0	0.077	0.0
0.4	0.014	0.015	0.030	0.0
0.5	0.006	0.287	0.010	0.001
0.6	0.003	0.678	0.006	0.084

3. Conclusions

The proton and helium GCR flux in the TeV range is described by a power law spectrum

$$\phi(E) = \phi_0 E^a$$

where α is around 2.7. Since helium nuclei weigh about four times as much as a protons, misidentified protons will contaminate the helium spectrum at an energy four time lower than their kinetic energy. Conversely, helium nuclei will contaminate the protons spectrum at an energy four time higher than their kinetic energy per nucleon. Because of the rapidly falling flux as a function of energy, measurement of the protons spectral slope will be more sensitive to contamination by helium than the reverse.

References

[1] J. H. Adams Jr., G. L. Bashindzhageyan, V. I. Zatsepin et al, Nuclear Instruments and Methods in Physics Research A, 524 (2004) 195-207.